Physica B 404 (2009) 1181–1186

Contents lists available at ScienceDirect

Physica B

journal homepage: www.elsevier.com/locate/physb

# Characterization of defect modes in one-dimensional photonic crystals: An analytic approach

N. Ansari [a], M.M. Tehranchi [a,b,*], M. Ghanaatshoar [a]

[a] Laser and Plasma Research Institute, Shahid Beheshti University, Evin, Tehran 1983963113, Iran
[b] Physics Department, Shahid Beheshti University, Evin, Tehran 1983963113, Iran

ARTICLE INFO

*Article history:*
Received 13 July 2008
Received in revised form
16 November 2008
Accepted 19 November 2008

*Keywords:*
Photonic crystals
Defect modes
Dispersion relation

ABSTRACT

We introduce an analytical model to investigate the localized defect modes associated with a defect cell inserted in a one-dimensional photonic crystal for both transverse electric (TE) and transverse magnetic (TM) polarizations, at an arbitrary angle of incidence. The defect cell, which is made of two dielectric constituents, leads to the appearance of several localized defect modes within the photonic band gaps. We develop an analytical approach based on the both transfer matrix and Green's function methods to determine the number and frequency of the defect modes that can be controlled easily by varying the parameter values of the constituent layers of the photonic crystal. The method demonstrates that the electric field amplitude depends on the defect cell position in the photonic crystal while the defect mode frequency is independent of it. This method is useful for photonic band gap engineering and designing the photonic-based devices.



## 1. Introduction

During the last few decades, starting from the pioneering work of Yablonovitch [1] and John [2], photonic band gap (PBG) materials or photonic crystals (PCs) have received considerable attention for fundamental physics studies as well as for potential applications in photonic devices [3–5]. The main attraction of PCs is the existence of forbidden band gaps in their transmission spectra.

The perfect PC has many applications, but its doped versions may be more useful, as semiconductors doped by impurities are more important than the pure ones. Due to the important role of defects in technical applications, they have been studied extensively in PCs [6]. The defects have also attracted considerable attention in other materials possessing spatial periodicity such as plasmonic crystals [7], phononic crystals [8] and magnonic crystals [9,10].

A defective PC is constructed by introducing a disorder into the regular structure of the PC. For instance, in a one-dimensional (1D) PC, the defect is a layer different in nature (materials and size) from the other layers. By inserting a defect into a PC, it is possible to create highly localized defect modes within the PBG. Such defect modes are localized at the position of the defect. The control of defect modes is of major interest for their application in narrow band filters [11,12] and low threshold lasers [13,14]. However, the design of controllable defect modes in PCs requires predictive formulae for dependence of the defect mode frequencies on physical parameters of PCs and on the angle of incident light. Conducting even numerical investigations such as frequency difference time domain [15,16] and plane wave expansion [17] on PBG defect problems still remain a challenge for two- and three-dimensional PCs; therefore, 1D PCs are common choices for analytical investigations because of their simplicity.

There are some analytical techniques for defect mode frequencies in 1D PCs such as the interface response theory [6] and Bloch wave approximation [18]. A closure formula for defect mode frequencies can also be derived using the transfer matrix method (TMM) [19], which is usually utilized to calculate the transmission and reflection coefficients of incident electromagnetic waves. In this order, besides applying boundary conditions at each interface between PC layers, supplementary equations, which are provided regarding the physical conditions in the PC, are applied to obtain a closure formula. For instance, in the perfect PC, the dispersion relation can be obtained using the transmission and reflection spectra derived from TMM and simultaneously applying the Bloch condition. In a defective PC, the Bloch condition is not fulfilled and other supplementary equations such as zero condition for reflection spectra [20] or boundedness condition [21] should be employed. A simple equation was first proposed by Ozbay and Temelkuran [23] to study defect modes in a 1D PC and has been developed recently by Nemec et al. [22]. The method is based on

* Corresponding author at: Laser and Plasma Research Institute, Shahid Beheshti University, Evin, 1983963113 Tehran, Iran. Tel.: +98 21 22431773; fax: +98 21 22431775.
*E-mail addresses:* Teranchi@cc.sbu.ac.ir, mmteranchi@yahoo.com (M.M. Tehranchi).

0921-4526/$ - see front matter Crown Copyright © 2008 Published by Elsevier B.V. All rights reserved.
doi:10.1016/j.physb.2008.11.093

the application of the total reflection of a perfect PC and quantities that can be determined experimentally. This method is applicable only for the defect located at the center of a perfect PC. On the other hand, these conditions can explain some experimental situations but each of them represents a reduction of generality. To our knowledge, there is no TMM-based analytical report regarding more general calculations of defect mode frequencies in defective PCs.

In this study, using TMM, we develop an analytical method for calculating the defect mode frequencies with less limitations. In this order, by applying boundary conditions for electric and magnetic fields of the electromagnetic waves at the interface between PC layers and implementing some mathematical procedures, a recursion relation for the electric field at the surface of each unit cell can be obtained. We will show that it is possible to write this relation as the sum of two terms; one of them is merely related to the perfect PC and the other one is due to the existence of the defect. Subsequently, considering an infinite PC and applying Green's function method, an analytical relation for defect frequencies can be deduced. In comparison with the results of TMM, it will be shown that we do not lose the generality by the assumption of an infinite PC. The method allows us to investigate analytically the dependence of defect mode frequency and electric field amplitude on the defect cell position. We apply this method to a 1D PC consisting of periodically repeated bilayer cells perturbed by a defect cell. We consider general conditions that include non-absorbing and non-dispersing isotropic dielectric materials, and calculate the PBG and defect mode frequencies for both transverse electric (TE) and transverse magnetic (TM) polarizations at various angles of incidence.

## 2. Theoretical description

Let us consider an infinite 1D PC comprising the periodically repeated thin layers of two types, i.e. …*ABABAB*… The layered structure is periodic in the $z$ direction and homogenous in the $x$–$y$ plane. The layers are characterized by their thicknesses, $d_A$ and $d_B$, and their refractive indices, $n_A$ and $n_B$, respectively, and $L = d_A+d_B$ is the length of periodicity of the PC. A defect is modeled as a double layer inserted into the PC, as shown in Fig. 1. The thicknesses of the defect constituent layers are $d_X$ and $d_Y$, and their refractive indices are $n_X$ and $n_Y$. This model also allows for the treatment of two different types of single-layer defect: (a) when the thickness of one of the defect layers is equal to zero, the model describes a "defect of insertion", i.e. …*ABABAB*…, and (b) when the thickness and refractive index of one of the defect layers are identical to those of the non-neighboring PC's normal layer, the model describes a "defect of replacement", i.e. …*ABABAB*… The latter establishes a defective symmetric PC with respect to the defect layer position.

Let a plane wave be injected from vacuum into the PC as shown in Fig. 1. In this case, the electric field can be written as

$$\mathbf{E}(x,z) = (c_J^+ e^{ik_J \cos\theta_J z} + c_J^- e^{-ik_J \cos\theta_J z}) e^{ik_J \sin\theta_J x}, \quad (1)$$

in which the magnitude of wave vector, $\mathbf{k}_J = k_J \sin\theta_J \hat{x} + k_J \cos\theta_J \hat{z}$, for a wave with a frequency of $\omega$ propagating in the $J$th layer (i.e. $J = A,B,X$ and $Y$) with a refractive index of $n_J$, is $k_J = \omega n_J/c$ where $c$ is the speed of light in vacuum. In Eq. (1), $c_J^+$ ($c_J^-$) is the amplitude vector of the incident (reflected) electric field and $\theta_J$ is the propagation angle in the $J$th layer. Using the Maxwell equations and Eq. (1), a similar equation for the magnetic field can be derived. For the TE (TM) wave the electric field **E** (the magnetic field **H**) is in the $y$ direction. At the interface of adjacent layers, the tangential components of **E** and **H** should be continuous. It has been derived that **E** and **H** just before the $I$th unit cell are related by the transfer matrix $T_I$ to those just before

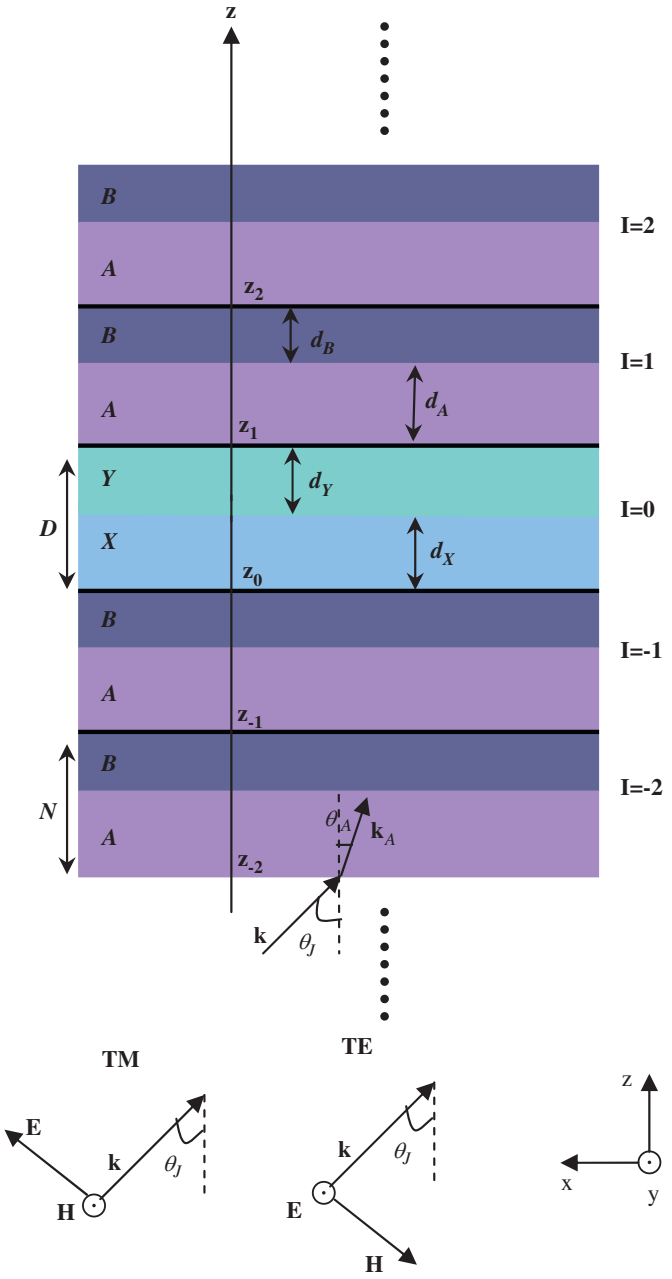


**Fig. 1.** Schematic of 1D PC with a defect cell. A defect cell, $D$, consisting of binary $X$ and $Y$ layers is located in $I = 0$. The other cell, $N$, consists of alternative $A$ and $B$ layers. Here, $\theta_J$ is the incident angle, **k** is the incident wave vector, **E** is the electric field and **H** is the magnetic field. The plane of the incidence is the $x$–$z$ plane.

the next unit cell [24]. We label the transfer matrix for a normal cell, $T_N$ ($I \neq 0$) and for the defective cell, $T_D$ ($I = 0$). The transfer matrix for a normal cell is given by

$$T_N = \begin{bmatrix} \lambda_N & \sigma_N \\ \zeta_N & \mu_N \end{bmatrix}, \quad (2)$$

in which

$$\lambda_N = \cos\alpha\cos\beta - \frac{p_A}{p_B}\sin\alpha\sin\beta, \quad (3a)$$

$$\sigma_N = -i\left(\frac{1}{p_A}\sin\alpha\cos\beta + \frac{1}{p_B}\cos\alpha\sin\beta\right), \quad (3b)$$

$$\zeta_N = -i(p_A\sin\alpha\cos\beta + p_B\cos\alpha\sin\beta), \quad (3c)$$

$$\mu_N = \cos\alpha\cos\beta - \frac{p_B}{p_A}\sin\alpha\sin\beta, \tag{3d}$$

where $\alpha = k_A\cos\theta_A d_A$ and $\beta = k_B\cos\theta_B d_B$. In Eqs. (3a)–(3d), $p_A$ and $p_B$ are as follows:

$$p_A = \frac{n_A\cos\theta_A}{c\mu_0}, \quad p_B = \frac{n_B\cos\theta_B}{c\mu_0} \quad \text{for TE mode}$$

and

$$p_A = \frac{1 \quad n_A}{c\mu_0\cos\theta_A}, \quad p_B = \frac{1 \quad n_B}{c\mu_0\cos\theta_B} \quad \text{for TM mode}$$

where $\mu_0$ is the magnetic permeability of vacuum. The transfer matrix $T_D$ related to the defect cells can also be written similarly as

$$T_D = \begin{bmatrix} \lambda_D & \sigma_D \\ \zeta_D & \mu_D \end{bmatrix}, \tag{4}$$

where the matrix elements are defined by Eqs. (3a)–(3d) in terms of parameters relevant to the defect layers.

Using the transfer matrix in a general case, we can write

$$\begin{bmatrix} E_{I+1} \\ H_{I+1} \end{bmatrix} = T_I \begin{bmatrix} E_I \\ H_I \end{bmatrix} \tag{5}$$

in which

$$T_I = \begin{bmatrix} \lambda_I & \sigma_I \\ \zeta_I & \mu_I \end{bmatrix} \tag{6}$$

is the generalization of Eqs. (2) and (4). Combining Eq. (1) and Eq. (5), for the electric field, a similar equation for the magnetic field, the following recursion relation governing the electric field amplitude at interfaces of the adjacent unit cells can be obtained [8] as follows:

$$\frac{1}{\sigma_I}E_{I+1} + \frac{1}{\sigma_{I-1}}E_{I-1} = \left[\frac{\lambda_I}{\sigma_I} + \frac{\mu_{I-1}}{\sigma_{I-1}}\right]E_I. \tag{7}$$

Definitely, for a PC consisting of only normal cells, Eq. (7) is reduced to

$$E_{I+1} + E_{I-1} = (\lambda_N + \mu_N)E_I. \tag{8}$$

In a structure with an infinite number of layers, translational symmetry along the direction perpendicular to the layers leads to Bloch wave solutions of the form

$$E_\kappa(x,z) = E_\kappa(z)e^{i\kappa z}e^{ik_j\sin\theta_j x},$$

where $E_\kappa(z)$ is periodic with a period of length $L$, and $\kappa$ is the Bloch wave number given by the solution of the following equation [19]:

$$2\cos(\kappa L) = \lambda_N + \mu_N \equiv F_N(\omega). \tag{9}$$

If $|F_N|<2$, the wave number of the propagating Bloch wave is real but when $|F_N|>2$, $\kappa$ constitutes an imaginary part and the Bloch wave will be evanescent. The latter case corresponds to the so-called forbidden bands of the periodic medium and therefore the band edges of the PC can be determined by the use of the condition $|F_N| = 2$.

The dispersion relation of a PC containing a defect cell may be obtained by Eq. (7), which may be written as

$$(1+\delta K_I)E_{I+1} + (1+\delta K_{I-1})E_{I-1} = (F_N + \delta J_I + \delta M_{I-1})E_I, \tag{10}$$

where

$$\delta K_I = \delta K\delta_{I,0} = \left[\frac{\sigma_N}{\sigma_D} - 1\right]\delta_{I,0},$$
$$\delta J_I = \delta J\delta_{I,0} = \sigma_N\left[\frac{\lambda_D}{\sigma_D} - \frac{\lambda_N}{\sigma_N}\right]\delta_{I,0},$$
$$\delta M_I = \delta M\delta_{I,0} = \sigma_N\left[\frac{\mu_D}{\sigma_D} - \frac{\mu_N}{\sigma_N}\right]\delta_{I,0}. \tag{11}$$

Note that $\delta K_I$, $\delta J_I$ and $\delta M_I$ are non-zero only at the defect cell, i.e. for $I = 0$. In order to solve Eq. (10) we formally express it as

$$\sum_h (L_{Ih} + \delta L_{Ih})E_h = 0, \tag{12}$$

where

$$L_{Ih} = \delta_{I,h-1} + \delta_{I,h+1} - F_N\delta_{I,h},$$
$$\delta L_{Ih} = \delta K(\delta_{I,0}\delta_{I,h-1} + \delta_{I,1}\delta_{I,h+1}) - (\delta J\delta_{I,0} + \delta M\delta_{I,1})\delta_{I,h}. \tag{13}$$

Eq. (12), in the case of a perfect PC, will reduce to

$$\sum_h L_{Ih}E_h = 0. \tag{14}$$

Therefore, in Eq. (12) the term related to the defect has been completely separated. Now, we introduce Green's function $G_{Ih}$, similar to that in Ref. [25], defined by

$$\sum_m L_{\mathrm{Im}}G_{mh} = \delta_{I,h} \tag{15}$$

or equivalently by

$$G_{(I+1)h} + G_{(I-1)h} - F_N G_{Ih} = \delta_{I,h}. \tag{16}$$

For an ideal perfect PC, expanding $G_{Ih}$ in a Fourier series will then result in Ref. [23]

$$G_{Ih}(F_N) = \frac{1}{\pi}\int_0^\pi \frac{\cos[(I-h)q]}{2\cos q - F_N}\,dq = g_{I-h}(F_N). \tag{17}$$

Here, integration in Eq. (17) has a closed form only if $|F_N|>2$ [9]; therefore, from here we assume the condition to be fulfilled. For a PC with $(I-1)$ normal cells on either side of the defect cell, Eq. (12) may be written as

$$(\underline{1} + \underline{G}\,\delta\underline{L})\mathbf{E} = 0, \tag{18}$$

where $\underline{G}$ and $\delta\underline{L}$ are $2I\times 2I$ matrices with elements $G_{Ih}$ and $\delta L_{Ih}$, respectively, and $\underline{1}$ is the $2I\times 2I$ unit matrix. In Eq. (18), $\mathbf{E}$ is the $2I$–component column vector

$$\mathbf{E} = [E_{-I+1} \quad \cdots \quad E_{-1} \quad E_0 \quad E_1 \quad \cdots \quad E_I]^t, \tag{19}$$

where $t$ represents the transposition of a vector. It is easy to show that $\delta\underline{L}$ has only four non-vanishing components and can be written as

$$\delta\underline{L} = \begin{bmatrix} \underline{0} & \underline{0} & \underline{0} \\ \underline{0} & \delta\underline{l} & \underline{0} \\ \underline{0} & \underline{0} & \underline{0} \end{bmatrix} \tag{20}$$

in which the $2\times 2$ matrix $\delta\underline{l}$ is introduced in the form of

$$\delta\underline{l} = \begin{bmatrix} -\delta J & \delta K \\ \delta K & -\delta M \end{bmatrix}. \tag{21}$$

Moreover, the matrix $\underline{G}$ is partitioned in the same fashion,

$$\underline{G} = \begin{bmatrix} \underline{G}_{11} & \underline{f} & \underline{G}_{13} \\ \underline{f}^t & \underline{g} & \underline{h}^t \\ \underline{G}_{13}^t & \underline{h} & \underline{G}_{33} \end{bmatrix}, \tag{22}$$

where $\underline{f}$, $\underline{g}$ and $\underline{h}$ are $(I-1)\times 2$, $2\times 2$ and $(I-1)\times 2$ matrices, respectively, defined as

$$\underline{f}=\begin{bmatrix} g_{I-1} & g_I \\ \vdots & \vdots \\ g_1 & g_2 \end{bmatrix},\ \underline{h}=\begin{bmatrix} g_2 & g_1 \\ \vdots & \vdots \\ g_I & g_{I-1} \end{bmatrix},\ \underline{g}=\begin{bmatrix} g_0 & g_1 \\ g_1 & g_0 \end{bmatrix}. \tag{23}$$

Using the quantities given by Eqs. (20–23), Eq. (18) reduces to

$$(\underline{1}+\underline{g}\,\delta\,\underline{l})\begin{bmatrix} E_0 \\ E_1 \end{bmatrix}=0, \tag{24}$$

$$\begin{bmatrix} E_{-I+1} \\ \vdots \\ E_{-1} \end{bmatrix}=-\underline{f}\,\delta\,\underline{l}\begin{bmatrix} E_0 \\ E_1 \end{bmatrix} \tag{25}$$

and

$$\begin{bmatrix} E_2 \\ \vdots \\ E_I \end{bmatrix}=-\underline{h}\,\delta\,\underline{l}\begin{bmatrix} E_0 \\ E_1 \end{bmatrix}, \tag{26}$$

where $\underline{1}$ is now a $2\times 2$ unit matrix.

Solving Eq. (24) will determine electric field amplitudes at interfaces between the defect cell and the host cells and the defect mode frequencies. Eq. (24) may then be written as

$$\begin{bmatrix} 1-g_0\delta J+g_1\delta K & -g_1\delta M+g_0\delta K \\ -g_1\delta J+g_0\delta K & 1-g_0\delta M+g_1\delta K \end{bmatrix}\begin{bmatrix} E_0 \\ E_1 \end{bmatrix}=\begin{bmatrix} 0 \\ 0 \end{bmatrix}. \tag{27}$$

The solvability condition for this equation, i.e. $\det(\underline{1}+\underline{g}\,\delta\,\underline{l})=0$, leads, after some algebra, to

$$1+\delta K=0, \tag{28}$$

$$g_0F_D-g_1(\lambda_N\mu_D+\lambda_D\mu_N-\sigma_N\zeta_D-\sigma_D\zeta_N)=0, \tag{29}$$

where $F_D=\lambda_D+\mu_D$. Using Eq. (17), $g_0$ and $g_1$ are given by

$$g_0=\mp\frac{1}{\sqrt{F_N^2-4}}, \tag{30a}$$

$$g_1=\mp\frac{1}{\sqrt{F_N^2-4}}\left(\frac{\mp\sqrt{F_N^2-4}+F_N}{2}\right), \tag{30b}$$

where the minus (plus) sign is applied for $F_N>2$ ($F_N<-2$). Eq. (28) results in $\sigma_N=0$, which leads to a singularity in Eq. (7). Hence, the frequency satisfying $\sigma_N=0$ does not turn out to be a reasonable answer and therefore must be excluded.

The integral in Eq. (17) is responsible for $F_N>2$. This condition is precisely related to the region where the PBG appears for a perfect PC. Thus, each defect mode frequency is located only in the PBGs. Consequently, for an arbitrary direction of propagation, Eq. (29) determines the frequencies and the number of localized modes in each PBG with respect to the parameters of the PC and bilayer defect and Eq. (9) gives the allowed modes of Bloch wave propagation, $F_N<2$.

The electric field amplitudes for defect mode frequencies at interfaces away from the defect cell can be determined by Eqs. (25) and (26) in terms of $E_0$ and $E_1$. They can be written as

$$\begin{aligned} E_I &= g_I(\delta JE_0-\delta KE_1)+g_{I-1}(-\delta KE_0+\delta ME_1), \\ E_{-I+1} &= g_I(-\delta KE_0+\delta ME_1)+g_{I-1}(\delta JE_0-\delta KE_1). \end{aligned} \tag{31}$$

One can observe from this equation that the electric field amplitude decreases by moving away from the defect cell. According to Eq. (17) this is due to the reduction of $g_I$ when $I$ is increased.

In contrast to other methods [20–23], we can develop the above analytical formalism to investigate the effect of moving defect cell position on the field and the frequency of the defect modes. To study such effects, we assume the defect cell to be located in layer $I=j$. Thus, $\delta_{I,0}$ in Eq. (11) changes in $\delta_{I,j}$, and Eq. (13) can be rewritten as

$$\delta L_{Ih}=\delta K(\delta_{I,j}\delta_{I,h-1}+\delta_{I,j+1}\delta_{I,h+1})-(\delta J\delta_{I,j}+\delta M\delta_{I,j+1})\delta_{I,h}. \tag{32}$$

One can find that matrix elements of $\delta\,\underline{l}$ do not change because of these replacements, but their locations in $\delta\,\underline{L}$ change. Furthermore, $\underline{f}$, $\underline{g}$ and $\underline{h}$ of Eq. (23) are replaced by $\underline{f}'$, $\underline{g}'$ and $\underline{h}'$, respectively, with dimensions of $(I+j-1)\times 2$, $2\times 2$ and $(I-j-1)\times 2$, respectively, and can be written as

$$\underline{f}'=\begin{bmatrix} g_{I+j-1} & g_{I+j} \\ \vdots & \vdots \\ g_1 & g_2 \end{bmatrix},\quad \underline{h}'=\begin{bmatrix} g_2 & g_1 \\ \vdots & \vdots \\ g_{I-j} & g_{I-j-1} \end{bmatrix},\quad \underline{g}'=\underline{g}=\begin{bmatrix} g_0 & g_1 \\ g_1 & g_0 \end{bmatrix}. \tag{33}$$

Finally, using such replacements, Eqs. (24)–(26) can be rewritten as

$$(\underline{1}+\underline{g}\,\delta\,\underline{l})\begin{bmatrix} E_j \\ E_{j+1} \end{bmatrix}=0, \tag{34}$$

$$\begin{bmatrix} E_{-I+1} \\ \vdots \\ E_{j-1} \end{bmatrix}=-\underline{f}'\delta\,\underline{l}\begin{bmatrix} E_j \\ E_{j+1} \end{bmatrix} \tag{35}$$

and

$$\begin{bmatrix} E_{j+2} \\ \vdots \\ E_I \end{bmatrix}=-\underline{h}'\delta\,\underline{l}\begin{bmatrix} E_j \\ E_{j+1} \end{bmatrix}, \tag{36}$$

where $\underline{1}$ is now a $2\times 2$ unit matrix.

It is seen easily that Eq. (34) is similar to Eq. (24), which gives the defect mode frequency when the defect cell is located at $j=0$. Therefore, one can say that changing the defect cell position does not affect the defect mode frequency. On the other hand, Eqs. (35) and (36), which express electric field amplitudes for unit cells $-I+1$ and $I$, are different from Eqs. (25) and (26), which are corresponding equations when the defect cell is located at $j=0$. Therefore, the electric field amplitude varies by translating the position of the defect cell. Finally, it is found from Eqs. (35) and (36) that the highest transmission coefficient is obtained when the defect cell is fixed at $j=0$. That is because in this situation the elements of $\underline{f}'$ and $\underline{h}'$ matrices have their maximum values.

## 3. Results and discussion

As a model system, the $SiO_2$ and Si as dielectric materials of $A$ and $B$ were chosen, respectively. In our calculations, the thicknesses and the refractive indices are according to Ref. [26]. Therefore, the calculations were carried out using the values $n_A=1.5$, $n_B=3.7$, $d_A=234.9$ nm and $d_B=95.3$ nm. Applying Eqs. (9) and (29) and using the aforementioned parameters, the dispersion relation and the defect mode frequencies were calculated for the …*ABXAB*… structure. In this structure the defect layer was Si with a thickness of 220.6 nm.

Fig. 2 demonstrates the band structure for normal incident and shows that the defect mode frequencies are inside the PBGs. It can be seen that more than one defect mode may exist in a PBG. According to Eq. (29), the frequency and number of defect modes depend on the incident angle and both normal and defect layers

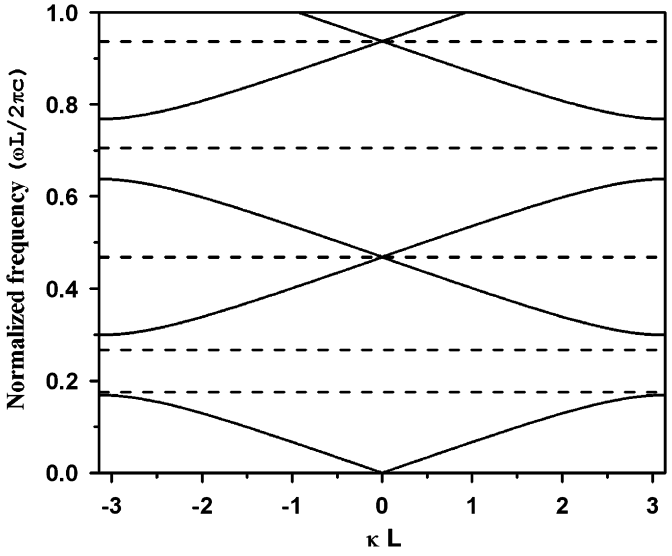


**Fig. 2.** Dispersion spectra of a 1D PC with a defect for the periodic structures of …$(SiO_2/Si)Si(SiO_2/Si)$… The calculations were carried out using $n_A = 1.5$, $n_B = 3.7$, $d_A = 234.9$ nm, $d_B = 95.3$ nm, $L = 330.2$ nm, $d_X = 220.6$ nm. Dashed lines represent the defect mode frequencies.

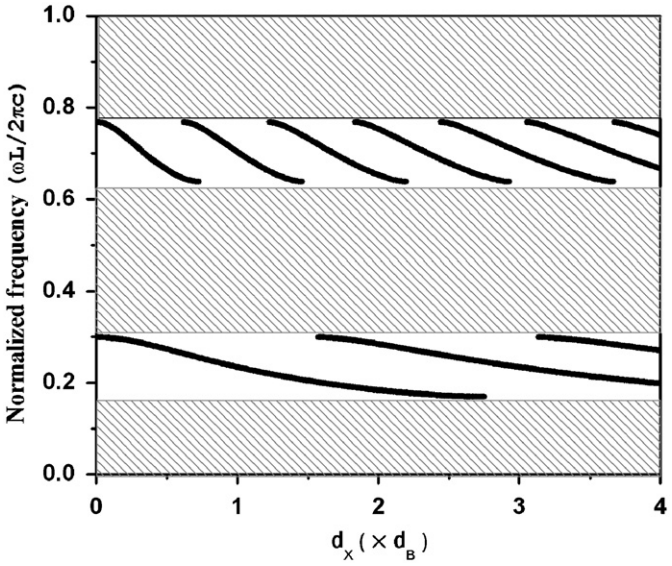


**Fig. 3.** The defect mode frequencies as a function of defect thickness (at $\theta_A = 0$).

parameters. It can be seen that the PBG width becomes zero where $\kappa L = 0$. As is well known, the defect mode frequency must appear only within the PBG. On the other hand, the defect mode frequency and PBG are degenerative for $\kappa L = 0$. However, it is not a general case and by changing the layer thickness at $\theta_A = 0$ or at different incident angles even in the same thickness, the PBG width does not become zero, and the degeneracy disappears where $\kappa L = 0$.

Fig. 3 shows the dependence of the number and frequencies of the localized modes upon the thickness of the defect layer. In this figure, the white areas represent the forbidden bands, the cross hatch areas are the propagation bands and the solid lines are the defect modes within the PBGs. As the defect thickness increases, the frequencies of the localized modes shift from the higher levels to the lower ones. Therefore, by varying the size of the defect cell, the defect mode frequencies can be adjusted within the band

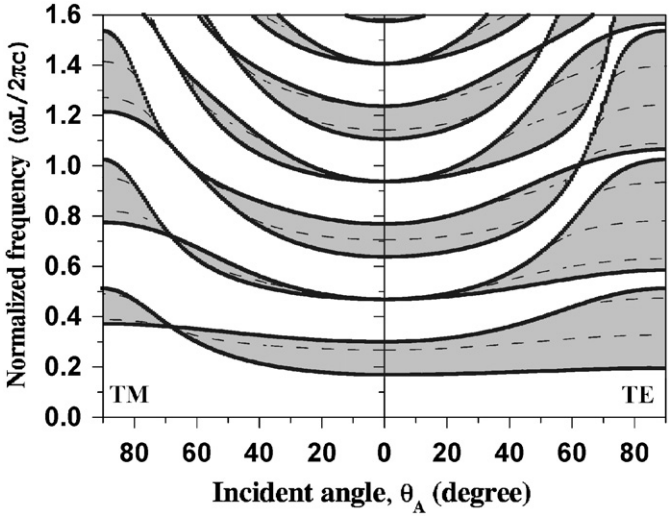


**Fig. 4.** Photonic band structures in terms of normalized frequency for the propagation angle $\theta_A$. The white areas represent the propagation bands and the gray areas are the forbidden bands.

gaps. This figure also indicates that the number of defect modes in a band gap can be controlled by thickness. As a result, we can find a range of thicknesses suitable for designing multi-frequency filters.

Fig. 4 shows the band gap regions and the defect mode frequencies as a function of propagation angle, $\theta_A$. In this figure, the gray regions represent the forbidden bands and the propagation bands are illustrated by the white areas. Defect mode branches can also be seen within the band gaps as dashed lines. This figure demonstrates that the number and frequency of defect modes change as the incident angle becomes higher. With increase in the oblique angle, the first gap of the TE mode increases; whereas that of the TM mode decreases up to Brewster angle and then increases again. At the Brewster angle ($\theta_{Br} = \tan^{-1}(n_B/n_A) \cong 67.93$), there is no reflection of TM waves and therefore the gap closes. There is no defect mode at the gap closing points. The number and position of TM closing points change for the higher gaps. There is no such closing point in the first band gap of the TE mode. However, there are some closing points in higher TE gaps. The closing points are useful to design the PCs for suitable applications. For example, knowing these closing points helps to create an omnidirectional reflector, operating in several distinct frequency ranges by using only a single PC [27,28].

The proposed analytical model determines the defect mode frequencies, the band gaps and the gap closing points for a variety of parameters of interest, including the defect layer thickness and the propagation angle. In order to have a comparison with a reference method, the calculation of defect mode frequencies for the $(AB)^N X(AB)^N$ structure has been carried out by TMM for $N = 1$, 2, 3 and 5. Both the defect mode frequencies and the band gaps calculated using this model are in very good agreement with those evaluated by TMM for $N = 5$ and at an arbitrary propagation angle. Therefore, the results of the two methods will exactly coincide with each other for large enough $N$ values. Consequently, we can conclude that by assuming of an infinite PC, we do not lose any generality.

## 4. Conclusion

The present paper has demonstrated an analytical study of the localized defect modes in the PBGs of a 1D PC at an arbitrary propagation angle for both TE and TM polarizations. This method

is able to derive an analytical closure formula to investigate the effect of the defect cell position on the defect mode frequency and electric field amplitude. We have found that changing the defect cell position does not affect the frequency of the defect mode, but strongly influences the electric field amplitude. The typical results of the proposed analytical approach for $\ldots(SiO_2/Si)Si(SiO_2/Si)\ldots$ show an excellent consistency with those derived using TMM. Furthermore, the effect of the defect layer thickness on the defect mode frequency has been investigated. We have shown that it can affect greatly the defect mode frequency. However, by comparison, this model can evaluate important quantities of the PCs, directly. This formalism may be applied to design photonic crystal-based devices.

## References

[1] E. Yablanovitch, Phys. Rev. Lett. 58 (1987) 2059.
[2] S. John, Phys. Rev. Lett. 58 (1987) 2486.
[3] C.M. Soukoulis, Photonic Band Gaps and Localization, NATO ARW, Plenum Press, New York, 1993.
[4] C.M. Soukoulis, Photonic Band Gap Materials, NATO ASI, Kluwer Academic Publishers, Dordrecht, 1996.
[5] J.D. Joannopoulos, R.D. Meade, J.N. Winn, Photonic Crystals, Princeton University Press, Princeton, 1995.
[6] J.-Q. Xi, M. Ojha, J.L. Plawsky, W.N. Gill, J.K. Kim, E.F. Schubert, Appl. Phys. Lett. 87 (2005) 031111.
[7] W.L. Barnes, A. Dereux, T.W. Ebbesen, Nature (London) 424 (2003) 824.
[8] J.O. Vasseur, B. Djafari-rouhani, L. Dobrzynski, A. Akjouj, J. Zemmouri, Phys. Rev. B 59 (1999) 13446.
[9] S. Tamura, Phys. Rev. B 39 (1989) 1261.
[10] V.V. Kruglyak, M.L. Sokolovskii, V.S. Tkachenko, A.N. Kuchko, J. Appl. Phys. 99 (2006) 08C906.
[11] V.I. Kopp, Z.-Q. Zhang, A.Z. Genack, Prog. Quantum. Electron. 27 (2003) 369.
[12] R. Wang, J. Dong, D.Y. Xing, Phys. Status Solidi 200 (1997) 529.
[13] L.J. Hodgkinson, Q.H. Wu, K.E. Torn, A. Lakhtakia, M.W. McCall, Opt. Commun. 184 (2000) 57.
[14] H. Yokoyama, M. Suzuki, Y. Nambu, Appl. Phys. Lett. 58 (1991) 2598.
[15] A.N. Kuchko, M.L. Sokolovskii, V.V. Kruglyak, Physica B 370 (2005) 73.
[16] M. Okano, A. Chutinan, S. Noda, Phys. Rev. B 66 (2002) 165211.
[17] K. Sakoda, H. Shiroma, Phys. Rev. B 56 (1997) 4830.
[18] Y.C. Tsai, K.W.K. Shung, S.C. Gou, J. Mod. Opt. 45 (1998) 2147.
[19] P. Yeh, Optical Waves in Layered Media, Wiley, New York, 2005.
[20] H. Nemec, L. Duvillaret, F. Quemeneur, P. Kuzel, J. Opt. Soc. Am. B 21 (2004) 548.
[21] A. Figotin, V. Gorentsveig, Phys. Rev. B 58 (1998) 180.
[22] H. Nemec, P. Kuzel, F. Garet, L. Duvillaret, Appl. Opt. 43 (2004) 1965.
[23] E. Ozbay, B. Temelkuran, Appl. Phys. Lett. 69 (1996) 743.
[24] M. Born, E. Wolf, Principles of Optics, seventh ed, Cambridge University Press, New York, 1999, p. 61.
[25] S. Tamura, H. Watanabe, T. Kawasaki, Phys. Rev. B 72 (2005) 165306.
[26] H.Y. Lee, H. Makino, T. Yao, A. Tanaka, Appl. Phys. Lett. 81 (2002) 4502.
[27] Y. Fink, J.N. Winn, S. Fan, C. Chen, J. Michel, J.D. Joannopoulos, E.L. Thomas, Science 282 (1998) 1679.
[28] J.N. Winn, Y. Fink, S. Fan, J.D. Joannopoulos, Opt. Lett. 23 (1998) 1573.